

Macroscopic Fundamental Diagram for Airplane Traffic Empirical Findings

Knoop, Victor L.; Ellerbroek, Joost; ter Heide, Mark; Hoogendoorn, Serge

DOI

[10.1177/03611981241265683](https://doi.org/10.1177/03611981241265683)

Publication date

2024

Document Version

Final published version

Published in

Transportation Research Record

Citation (APA)

Knoop, V. L., Ellerbroek, J., ter Heide, M., & Hoogendoorn, S. (2024). Macroscopic Fundamental Diagram for Airplane Traffic: Empirical Findings. *Transportation Research Record*.
<https://doi.org/10.1177/03611981241265683>

Important note

To cite this publication, please use the final published version (if applicable).
Please check the document version above.

Copyright

Other than for strictly personal use, it is not permitted to download, forward or distribute the text or part of it, without the consent of the author(s) and/or copyright holder(s), unless the work is under an open content license such as Creative Commons.

Takedown policy

Please contact us and provide details if you believe this document breaches copyrights.
We will remove access to the work immediately and investigate your claim.

Green Open Access added to TU Delft Institutional Repository

'You share, we take care!' - Taverne project

<https://www.openaccess.nl/en/you-share-we-take-care>

Otherwise as indicated in the copyright section: the publisher is the copyright holder of this work and the author uses the Dutch legislation to make this work public.

Macroscopic Fundamental Diagram for Airplane Traffic: Empirical Findings

Victor L. Knoop¹ , Joost Ellerbroek² , Mark ter Heide¹ ,
and Serge Hoogendoorn¹ 

Transportation Research Record
1–11

© The Author(s) 2024

Article reuse guidelines:

sagepub.com/journals-permissions

DOI: 10.1177/03611981241265683

journals.sagepub.com/home/trr



Abstract

For car traffic it was found that a more crowded area leads to a lower speed and a lower arrival rate. The relation between crowdedness and speed (or arrival rate) can be expressed in a network fundamental diagram, or macroscopic fundamental diagram (MFD). Similar concepts have been shown for pedestrian and train traffic. In this paper, we extend the concept to three spatial dimensions. While simulations have explored some concepts, we present for the first time empirical results of the relation between the crowdedness in the air and the performance of the “network.” We base our results on several months of data of airplanes around Amsterdam Schiphol Airport. Similar to car traffic, we observe a reduction in speeds as the number of airplanes in the area increases. However, even at the highest observed densities, we do not see a reduction in flows. This is because of active and intensive management (based on departure/landing possibilities), comparable to perimeter control in traffic, as well as a minimum airplane speed. This paper introduces an interesting concept of applying a MFD to three-dimensional (3D) spaces. We also show to what extent the performance reduction is caused by speed reduction and to what extent it is caused by less efficient routes. The MFD concept can eventually be used to also manage 3D airspaces for applications with less strict microscopic air traffic management than the current management around airports.

Keywords

operations, multimodal traffic, traffic flow

Air traffic as mode of transportation has been rising rapidly over the past decades (for example, Statistica [1]), which has increased the number of airplanes. Despite the many differences, it is interesting to compare aviation traffic to car traffic. Because of the large number of cars present, car traffic management often uses modeling and control approaches that describe traffic on an aggregated level. This means that there is no need to describe each individual vehicle. For car traffic, models and control are developed on different levels of description. There is the microscopic level, which models and controls individual cars. There is also the aggregated level, a macroscopic level, or even a network level, in which traffic is described at the road level or the network level, without considering individual vehicles. This is in line with, for instance, fluid dynamics where not all individual particles are being modeled, but predictions are made on the level of a flow. At this level, models and control are made using the properties of the stream. Such a higher level of description becomes more relevant if the number of particles

increases. Since a continued rise in the numbers of airplanes is expected in air traffic, it is worthwhile to investigate the properties of the stream also for air traffic, using models derived from car traffic research. If applicable, these can form the basis for modeling and control at higher aggregate levels.

In the past decade and a half, area-based traffic management for car traffic has received an increasing amount of scientific attention. This boost of attention started with the publication by Daganzo (2) arguing there should be a relationship between the number of cars and their average speed *at the zone level* (i.e., exceeding the level of a single road; one can think of a city center). Moreover,

¹Civil Engineering, Transport & Planning, Delft University of Technology, the Netherlands

²Aerospace Engineering, Delft University of Technology, the Netherlands

Corresponding Author:

Victor L. Knoop, v.l.knoop@tudelft.nl

Daganzo posed that because of the decreasing speed of the cars with increasing densities in the zone, the flow (also called production for a zone) should have a maximum point at some density. The relation between average speed and density in a zone has since then been referred to as a macroscopic fundamental diagram (which we will be using in this paper, abbreviated MFD), or (equivalent) a network fundamental diagram. For road traffic the flow–density relationship presented in the MFD is typically non-linear, where flow increases with density up until a certain critical value. Increasing density beyond this critical value leads to a reduction in flow, and an increase in overall travel time. Since then, many papers have started working on control schemes that keep the density in a zone below this critical density (e.g., Keyvan-Ekbatani et al. [3]) Interestingly, Daganzo (2) already mentioned that the concept of reduced speed with increasing density of particles (of whatever kind) would not only hold for road traffic, but many other processes, even including “your desktop.”

A significant part of air traffic management (ATM) consists of air traffic controllers managing individual flights, to keep them at safe distance from each other. In current-day ATM, air traffic is also managed at the flow level (through a process called air traffic flow management, ATFM), which is meant to ensure that the capacity of airports (and to some extent airspace sectors) is not exceeded. The main regulation that ATFM can impose is a departure delay, which is why current ATM research is focusing on other approaches as well, to better accommodate the rise in air traffic. With the recent rising interest in urban aerial transportation, network-constrained air traffic is now also studied, for instance with models for local interactions such as intersections (4), or organization of the airspace using virtual tubes (5). Free-flowing intersection capacity is further investigated by Aarts et al. (6).

Recently, a couple of works have presented simulation to test whether large-scale traffic descriptions also work for air traffic, and, more specifically, whether a MFD can also be used for air transport to draw conclusions on capacity and throughput in a similar way to road transport. The first efforts by Cummings and Mahmassani (7) show that also in three-dimensional (3D) air (drone) traffic, a relationship between flow and density would emerge at the area level. (Note in this paper we will adopt the convention to count only spatial dimensions; when including time, the same concept would be called four-dimensional). Tereshchenko et al. (8) also shows MFDs for air traffic. This paper mentions the effective distance covered, using the great circle (shortest path) distance to represent non-straight paths. The work by Haddad et al. (9) utilizes the concept of a MFD to apply perimeter control in 3D airspace.

In this paper we present an empirical verification of the MFD for conventional air traffic. Firstly, the next section will give more background on the origin and the use of the MFD in car and air transportation. Key to note is that the papers discussing and exploiting a MFD for air traffic use (microscopic) simulations as a basis, and this MFD has not been empirically verified.

For car traffic, validation of the MFD using empirical data from Yokohama (10) has accelerated the use of the concept of the MFD, which has led to models at the zonal level and many control concepts. With the current work, we would like to address the absence of an empirical MFD for air traffic. We aim to show that the relationship between density and production holds in air traffic as well. This can form the basis for air traffic modeling on an aggregated level, which can ultimately be used in the design of new air traffic control concepts.

Air traffic with airplanes is fundamentally different from car traffic. Near airports, all airplanes need to land or depart from a limited number of runways. There is therefore a very centralized hotspot rather than a central business district with some spatial extension. Secondly, near airports, air traffic is microscopically controlled in a centralized manner. Therefore, inefficient traffic operations caused by drivers that block intersections or so on should not occur. Finally, a major difference is that airplanes have a non-zero minimum speed (some margin above the stall speed) below which they cannot operate. Contrary to cars, airplanes cannot reduce their speed under a certain threshold to wait for other airplanes because they would simply fall to the ground. Options to delay airplanes are flying (a little) slower or taking a detour. This happens a great deal at some airports.

To delay an (airborne) aircraft in the case of congestion, air traffic controllers can make use of four different strategies: The simplest strategy is *linear holding*, which corresponds to a reduction in speed while maintaining the original track. As described above, this strategy is limited by the minimum operating speed of aircraft. The second strategy, often applied at the entry points to terminal airspace (initial approach fixes, IAFs), is to put aircraft in a *holding stack*; that is, a circular or oval pattern that adds a fixed amount of delay for each full round in the stack. The third strategy, *tromboning*, is applied just before landing, where the flightpath of the aircraft is extended along the centerline of the runway. With the fourth strategy, *vectoring*, air traffic controllers delay an aircraft by deviating them from their original path by a fixed course change.

The application area of a MFD for airborne traffic will most likely lie in low-altitude airspace with many drones, possibly flying autonomously following collision avoidance or priority rules. This is a different use of

airspace than the current air traffic near airports. We would therefore not expect the same MFD to appear in this low-altitude drone traffic as we might find in conventional air traffic. The aim of this paper is to for the first time show empirical evidence of a MFD for 3D traffic. Therefore, in this paper we will answer two questions. The main question is: what does a MFD for air traffic near an airport look like? A subquestion related to this is how to best express the relevant variables for and MFD for air traffic, since the principles for delay (detour instead of slowing down) are fundamentally different.

The remainder of this paper is set up as follows. The next section first gives a more extensive scientific background on (empirical) MFDs and traffic control for both air traffic and MFD-related control for car traffic. Then, the *Methodology* section presents the methods we use to create the MFDs. The data we will be using is described in the *Data* section followed by the *Results and Discussion* section, which presents the MFDs and their interpretation (and comparison to car MFDs). The final section presents the conclusions and potential applications.

Literature Review

The main macroscopic variables in traffic engineering are flow (i.e., the amount of traffic passing by a point on the road in a unit of time), density (i.e., the number of vehicles per unit of space), and average speed. The difficulty is that flow and density are measured along different dimensions (one along time and one along space), which makes it impossible to rightfully relate flow and density in the same observation span to each other. Edie (11) presented his generalized definitions of traffic. He argued that flow, density, and speed could be measured over an arbitrary area in space-time. These have been the cornerstone for traffic engineering since. He defined the following:

$$\text{Flow (veh/h)} q = \frac{\text{Total distance covered (veh.km)}}{\text{Area in space} \times \text{time (km.h)}} \quad (1)$$

$$\text{Density (veh/km)} k = \frac{\text{Total time spent(veh.h)}}{\text{Area in space} \times \text{time (km.h)}} \quad (2)$$

$$\text{Speed (km/h)} v = \frac{\text{Total distance covered(veh.km)}}{\text{Total time spent (veh.h)}} \quad (3)$$

The elegance of these equations is that they simplify to the intuitive relations for flow and density either applied to a period of time at single location (measuring flow) or a single moment in time over a road stretch (measuring density). A natural extension applied in MFD-related works is to define the “area in space time” as the product of the aggregation interval, times *the total road length* in

the zone. For pedestrian traffic, a two-dimensional (2D) process, flow is similarly defined with the area as 2D space. This yields a flow in pedestrians per meter per hour, which can be interpreted by how many pedestrians pass by in one unit of time over 1 m of width of the road (typically perpendicular to the walking direction). The density is expressed in pedestrians per square meter. Extensions to 3D traffic, as well as our proposed extension for airplane traffic, follow in the next section.

Air traffic at and around airports is typically managed by the control tower. This tower has a complete overview of the gates, taxi-ways, and runways. The traffic is managed by air traffic controllers who are using visual and instrumental observations. The controlling system is based on flight progress strips. Such a strip contains individual flight information of the airplanes that are currently operating on the airport. The strips are categorized per operation status, for example: flights that have started up but have not started taxiing yet or flights that are in the taxi phase. These categories are designated to specific areas in the control tower. A specific air traffic controller is then responsible for a specific area. So air traffic is controlled at the individual level. Without the clearance of air traffic control, airplanes at or near controlled airports are not allowed to move around. In general, a ground delay program can assist this and keep aircraft on the ground to limit airborne holding (12).

As mentioned in the introduction, a couple of works have studied MFDs for 3D (drone) traffic, using simulation (7–9). As far as the authors are aware, no empirical works have been published, and none have studied MFDs for conventional airplane traffic.

For car traffic, the first speed–density relationships for a network were mentioned and shown by simulation in Godfrey (13) and Mahmassani et al. (14). Then, a revival of the concept started, as mentioned, by the realization that flow decreases when increasing density beyond a critical point (2), with the first empirical results presented by Geroliminis and Daganzo (10). Since then, many papers have followed on control, which we discuss below. The original paper from Geroliminis and Daganzo (10) used data from taxis in Yokohama.

Later works have, for instance, verified the concept using loop detector data (e.g., Knoop and Hoogendoorn [15]) or using data of all Android phones (16). This comes at a cost if not all vehicles are probed (17). Later studies have proposed to combine different data sources (18). The empirical validation of the concept of the MFD cumulated with the work of Loder et al. (19), showing an empirical MFD for more than 40 networks. Note that these empirical MFDs seldom show a properly “congested branch,” that is, a branch for which the total production decreases with a higher accumulation. This does happen quite often in simulations with extensive

loading, or because of instabilities that cause some parts of the network to become unstable (see, e.g., Gayah and Daganzo [20] and Hani Mahmassani and Zockaie [21]).

Also for other modes MFDs have been explored and presented. The most surprising might be the exploration of MFDs for train networks (22). Note that this is a proper network-wide MFD, and the paper explicitly indicates the differences with car traffic. More relevant to air traffic might be the work exploring and explaining MFDs for pedestrian traffic (e.g., Hoogendoorn et al. [23]). The similarity with air traffic is that pedestrians can be considered as “particles” that move in a continuous multi-dimensional space. For pedestrians, a MFD was found in empirics and a modeling form or explanation has been proposed. For further extensions of MFDs, including modeling and multiple interacting classes, we refer to the recent literature review by Johari et al. (24).

For car traffic, in the past decade various control schemes using the MFD have been proposed. Knoop et al. (25) proposed to route cars based on the crowdedness (and speed) in the network; the original responsive routing can also be applied in a model predictive control framework (26). This approach implicitly applies perimeter control, but at a section with multiple reservoirs. Perimeter control itself is pioneered by Geroliminis et al. (27) for a theoretical case and by Keyvan-Ekbatani et al. (3) for a realistic case with simulation. They both show that limiting the inflow to a zone can give large benefits with respect to total travel time. The aim in both cases is to not let the density exceed the critical density for a given zone. This has been further tuned, and extensions to this process still are the subject of study (e.g., control delays [28]).

Methodology

To obtain a MFD for conventional air traffic, we extend the concepts of Edie (11). As argued by Cummings and Mahmassani (7), in principle Edie’s definitions also apply to air traffic:

$$q = \frac{\text{Total distance covered (veh.km)}}{\text{Area in 3D-space} \times \text{time(m}^3\text{.h)}} \quad (4)$$

$$k = \frac{\text{Total time (veh.h)}}{\text{Area in 3D-space} \times \text{time(m}^3\text{.h)}} \quad (5)$$

Linear holding would reduce an airplane’s speed; the other mentioned delay strategies (vectoring, tromboning, and holding) involve path stretching. A better way of indicating the production of an airspace is the *effective distance covered*: the shortest path from the starting point of an aircraft to its destination. For airplanes we take the shortest path at a constant altitude. Since Earth is curved, the shortest path between two points is the so-

called great circle path, with the matching great circle distance. For the distance of a single airplane, we therefore define the production and density as follows:

$$P = \frac{\text{Total effective distance covered (veh.km)}}{\text{Area in 3D-space} \times \text{time (m}^3\text{.h)}} \quad (6)$$

$$= \frac{\sum_{\text{Allairplanes}} \text{Effective distance covered (veh.km)}}{\text{Area in 3D-space} \times \text{time (m}^3\text{.h)}}$$

$$k = \frac{\text{Total time (veh.h)}}{\text{Volume in 3D-space} \times \text{time (m}^3\text{.h)}} \quad (7)$$

$$= \frac{\sum_{\text{Allairplanes}} \text{Flying time in area (veh.h)}}{\text{Volume in 3D-space} \times \text{time (m}^3\text{.h)}}$$

In this equation, only the effective distance is taken into account toward the production. The resulting effective speed is the quotient of this effective distance and the total time spent traversing this distance:

$$v = \frac{P}{k} = \frac{\text{Total effective distance covered (veh.km)}}{\text{Total time spent (veh.h)}} \quad (8)$$

In this paper, we mix various disciplines with their own tradition of units. We will use the metric system to indicate flows (production), densities, and speed, since they are easier to relate to each other than mixing miles and knots. For altitude indications, we stick to feet (and flight levels, which are 100 ft) to maintain well-rounded values for the altitudes.

To construct a MFD, we take all flight movements in an area around an airport between altitudes of 5500 and 19,500 ft. We aggregate all movements (i.e., sum all effective distances and times spent) over a period of 30 min.

We will construct the figure of production versus density. Since the situation of an empty airspace means no density and no flow, the graph should start from the origin. Then a point cloud will show production. For car traffic, we know that production will reach an optimum (19). In simulated conditions, the flow might even reduce with increasing density because of gridlocks occurring (e.g., Gayah and Daganzo [20] and Daganzo et al. [29]). In those cases, vehicles block each other in a circular way, leading ultimately to the standstill of all vehicles. In practice, higher densities than the density matching the production is highest are seldom reached.

The gradient of a line from the origin to a point indicates the effective speed of the airplanes during that period. We can also express this effective speed of the airplanes in the aggregation interval, and show its relationship with density. We expect this to more clearly show differences in speed.

The effective speed for an empty airspace will be called free speed, in analogy with traffic engineering. Note that this is not the speed of an individual airplane, but can be

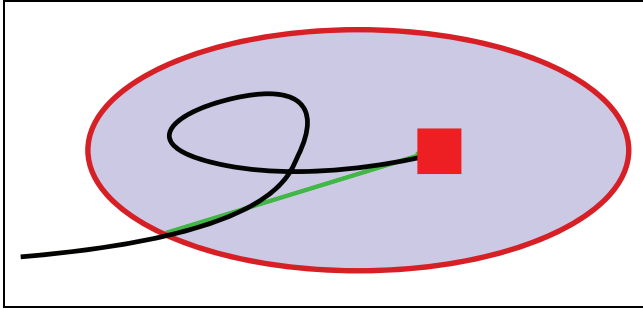


Figure 1. A considered area in space–time (blue shaded) and the hypothetical path of an airplane (black line) to an airport (red square). The green line denotes the effective distance.

Note: Color online only.

interpreted as the mean of the speed of all airplanes, and only considering the effective movements (see Figure 1). We will quantify the free-flow speed by finding the median speed of the low densities.

Now let us discuss efficiency. In the ideally effective world, airplanes would have no interference, and the effective speed would remain constant. We define efficiency as part of the production that is actually in the system compared to this ideal case:

$$\eta = \frac{P}{kv_{\text{free}}} \quad (9)$$

We will analyze the loss of efficiency with increasing density. Note that, because of our definition, this can come from airplanes flying slower, airplanes taking a longer route, or both. We will explicitly derive the origin of the loss of efficiency. This means that we will, besides the effective path length, also record the factual path length during each aggregation interval (see Figure 1). The ratio of the two shows which part of the loss of production is caused by the increase in path length, and therefore the other part is caused by the decrease in speed.

Let us note that speed for airplanes is more complex than speed for cars. The only relevant variable for car speed is the speed difference with the ground. For airplanes, its speed compared to the wind, the true air speed (TAS). This is related to ground speed. The difference between the ground speed and the TAS is the wind speed. Moreover, an airplane takes the indicated air speed (IAS) as reference. This is what the gauges indicate. This speed depends on the dynamic pressure of the airplane, and therefore depends, next to the TAS, on the air pressure and is therefore related to the altitude. When descending under constant IAS, the air pressure increases, so the TAS (and therefore the ground speed) will reduce. As a rule of thumb, the following can be used: $TAS = IAS + \text{flight level}/2$, in which units of knots and are used; the flight level is the altitude in 100 ft.

Therefore 200 knots IAS at FL250 (i.e., 25,000 ft; 370 km/h or 230 mph) equals (approximately) the same TAS as 325 knots (600 km/h or 375 mph) at ground level.

To illustrate (potentially small) changes in effective speed even more, we will also show how differences between effective speed and free speed relate to density. We expect that this difference will increase with increasing density.

Data

We will analyze the data for Amsterdam International Airport Schiphol (AMS). Schiphol is one of the busiest airports in Europe with around 72 million passengers per year, and approaching 500,000 airplane movements (pre-COVID numbers [30]). It is located in an almost level area, and there is no interference from geography with the flights. Because of the amount of data, we make a selection in months. We will be using all data from April and August 2019 (regular and holiday season, both pre-COVID-19), and from April and August 2020 (low flight numbers caused by COVID-19, with the low caused by COVID in April 2020). Typically, there are quiet periods during the night and more busy periods during the day with typical peaks. Figure 2 shows the number of airplanes in the considered area as function of the time of day. It shows that in the aggregation interval there are 60+ airplanes, which is sufficient to get a reliable estimate for flow and density. We also show the density of the airplanes based on these numbers. Note in this figure also the large effects of the COVID pandemic, with April 2020 having 87% fewer flights than April 2019.

The airspace near Schiphol is divided into three main categories. From small to large these are the controlled traffic zone (CTR), terminal maneuvering area (TMA), and control area (CTA). The CTR is the zone controlled by the air traffic control tower at the airport. In this airspace the initial departure and final approach take place. Air traffic controllers control this zone with direct visual observations and instrumental observations. The TMA is controlled only by instrumental observations, with air traffic controllers sitting in a control room. The TMA holds the departure and arrival routes. Holding stacks are typically placed at the edge of the TMA, alongside a limited number of initial approach fixes: fixed entry points into the TMA. CTA airspace is situated at altitudes above the TMA, and contains flights in cruise and flights transitioning to and from cruise flight.

We will be using the CTA since it includes the flights approaching and departing Schiphol airport. To include a sufficient area, we include the five Dutch CTAs combined (see Figure 3). We will be using only the data

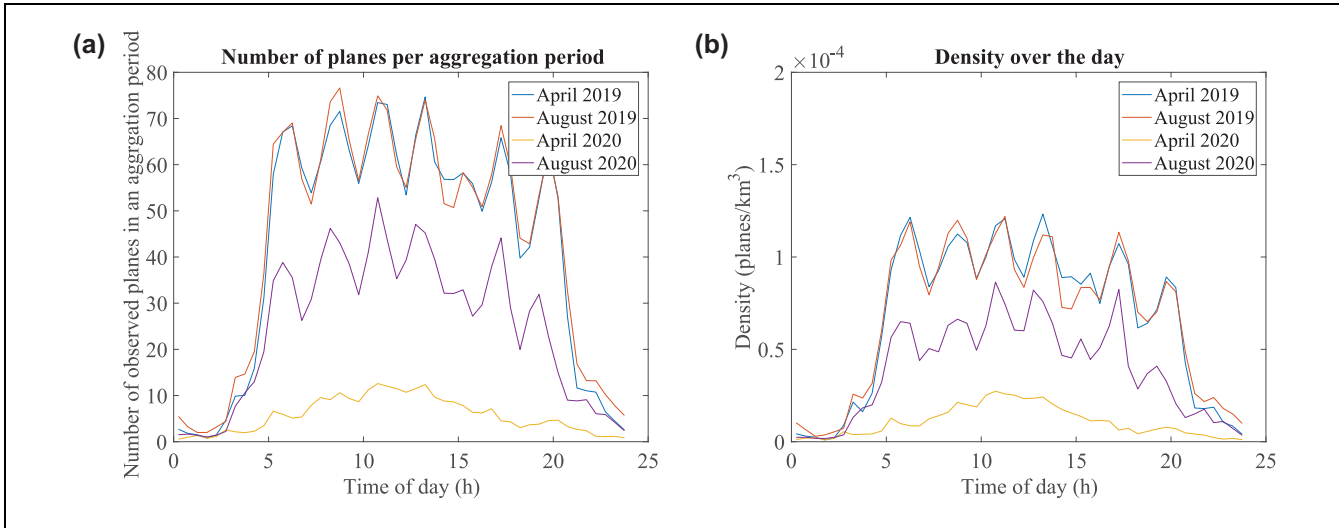


Figure 2. The distribution of flights over the day: (a) number of airplanes and (b) density.

between FL055 and FL195 (i.e., 5500 and 19,500 ft) to exclude airplanes crossing this area and not interacting with the maneuvering airplanes. Finally, note that the airspace consists not only of airplanes in- and outbound from Schiphol but also of airplanes heading to or from other airports relatively close by. Air traffic of airports Eindhoven, Rotterdam, and Düsseldorf also pass through the considered area, and will therefore also affect air traffic near Schiphol airport. Since the airplanes are within the airspace, they contribute to the density and flow of the considered area and are part of the analysis. On average, these flight account for 17% of the flights in the considered airspace (31).

The surface area of the considered area measures $42,807 \text{ km}^2$. The height is $19,500 \text{ ft} - 5500 \text{ ft} = 14,000 \text{ ft} = 4.28 \text{ km}$. The total volume therefore is $42,807 \times 4.28 = 182,667 \text{ km}^3$.

For this research we will be using data from the Automatic Dependent Surveillance-Broadcast (ADS-B). The data are recorded by a receiver at the top of the aerospace faculty building of the Delft University of Technology. Range is limited to the line-of-sight because of the curvature of Earth. The range is larger than the range required for this research and therefore does not a form limiting factor. These data contain the following for each airplane: ICAO aircraft address (unique ID), latitude, longitude, altitude, ground speed, track (degrees), and rate of climb. These data are periodically broadcast by every airplane equipped with an ADS-B transponder. Each message is time-stamped on reception.

We use the data to find the point and time of entry into the CTA at the desired altitude, and the point and time of entry out of the CTA at the desired altitude. We do so for every flight. An example with two airplanes is

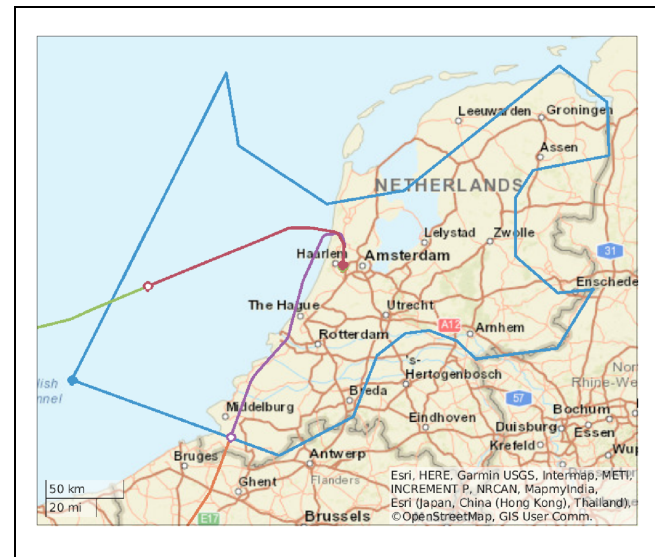


Figure 3. The considered area (control area, blue line) and two flight trajectories into Schiphol.

Note: Color online only.

shown in Figure 3. Note that there are several starts possible to be included in the considered data: while being at the right altitude once it crosses the boundary (the orange/purple line) or the while it is inside the CTA once it reaches the right altitude (green/red) line. Typically, the included parts of a flight are (1) a flight from the boundary to the airport or vice versa, (2) a flight from the boundary to the boundary, or (3) a flight from the boundary to a point in the area (or vice versa), or from the airport to a point in the area (or vice versa); this happens if the aggregation interval starts or ends in with the flight through the CTA.

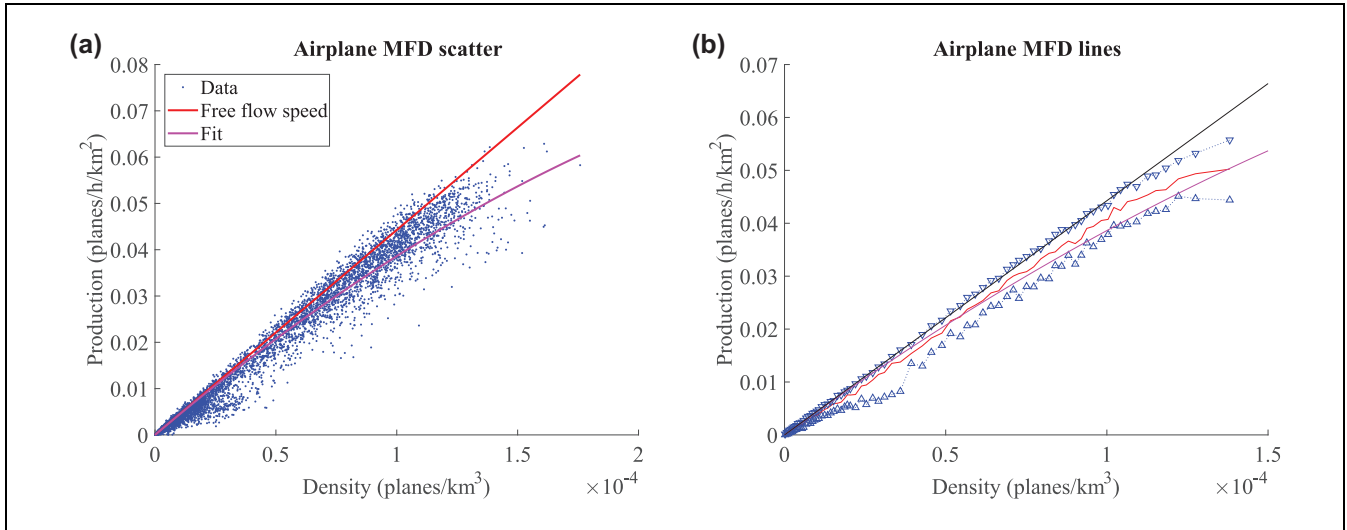


Figure 4. The macroscopic fundamental diagram (MFD) for airplanes: (a) scatter and (b) trends.

Note: Color online only.

Results and Discussion

Firstly, let us discuss the MFD presented in Figure 4. Figure 4, *a* and *b*, presents the same data in different ways. Figure 4*a* shows a scatter plot of the density versus production. It also shows (in red) a line with constant slope (free-flow speed, see below) and a fit of the data (in purple, see also below). Because the scatter plot does not clearly show the width of the point cloud, Figure 4*b* shows the same data, where we also express the data by a median line and 17 and 82 percentile values in blue. These values represent the inclusion of the mean and plus or minus 1 standard deviation in the case of a normal distribution.

The figures show an observed density range between 0 and approximately 0.0002 airplanes per cubic km. Let us first consider the range of the plot. The minimum separation to any other airplane is 5 nmi in each direction (9.62 km) in the horizontal airplane, and 1000 ft up and 1000 ft down (2×0.305 km). This means an airplane would need a disk for itself. The volume of this disk is $\pi(9.62)^2 \times 2 \times 0.305 = 177 \text{ km}^3$. If we could pack them without voids, a maximum density could be achieved of $1/177 = 0.0056$ airplanes/ km^3 . Since disks cannot be placed next to each other without voids, there is a packing inefficiency (when arranging the disks optimally in a hexagonal packing). Geometrically it can be derived that then only $(\pi\sqrt{3})/6 \approx 91\%$ of the space can be used. The maximum density then becomes $1/177 \times 0.91 = 0.0051$ airplanes/ km^3 . Note that this theoretical maximum can only be achieved if either all airplanes are stationary, or when all airplanes are flying at the same speed, in the same direction.

The found range to 0.0002 airplanes/ km^3 is indeed well below the theoretical maximum density if all airplanes were at their minimum separation.

As hypothesized we see that flow is increasing with density up to the highest densities reached. We do see, however, that the gradient of the relationship between effective production and density is decreasing with increasing density. This indicates that as densities go up, effective speeds reduce. The width of the distribution is notably smaller than the increase, indicating that the increase is significant. Moreover, the comparison of the constant speed line and the bounds of the MFD show that the reduction of effective speed is also beyond the natural fluctuations.

The speeds are also shown in Figure 5 with the same line styles and colors as Figure 4. At very low densities, we see a high variability in speeds. This is because these densities are observed in situations where only a part of the trajectory of a single flight falls into the area of interest. For instance, an airplane takes off at 5.29 a.m. and no flights have been recorded earlier. Then, only the first minute of that flight falls into the aggregation area. The effect is similar for take-offs or for airplanes crossing the CTA. All in all, the aggregation areas with very low density are not very reliable. We therefore set the free-flow speed as the mean of the average speed of percentiles 3–8. We found the percentiles by checking the lowest percentiles where the free-flow speed becomes constant. We find a free-flow speed of 442 km/h (239 knots). Note that this is close to the CTA procedural maximum speed of 250 knots.

The red line in Figure 4 indicates the free-flow speed. It is clear that the effective speed of the airplanes reduces

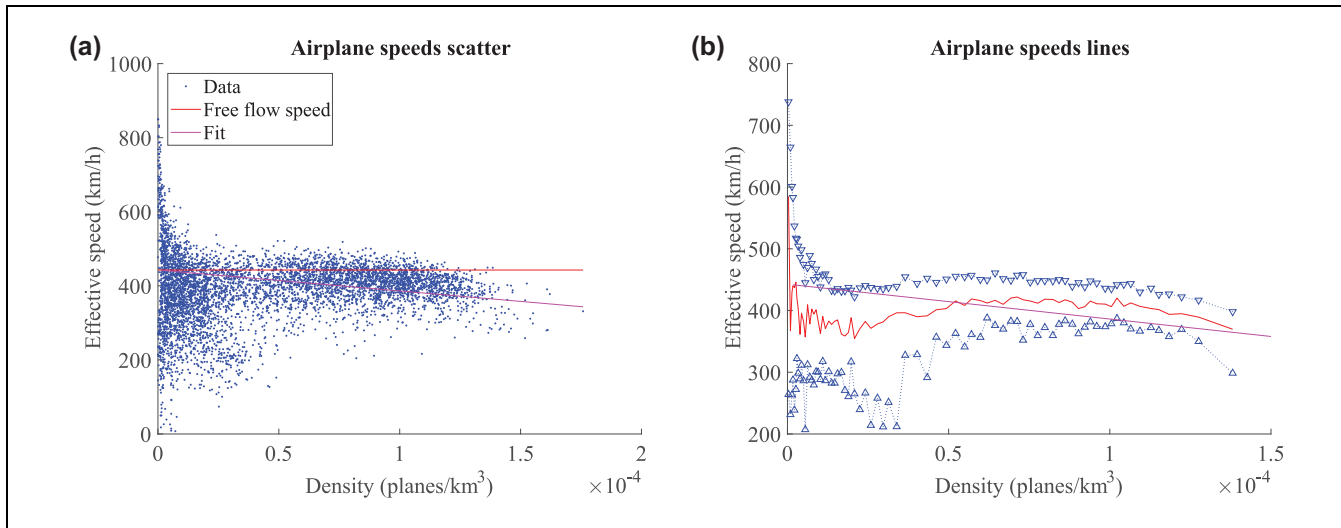


Figure 5. The effective speed of airplanes: (a) scatter and (b) trends.
Note: Color online only.

with density. We therefore also show a fit of the MFD according to a linearly decreasing speed. Fitting a fundamental diagram is not trivial, and a good approach is fixing some degrees of freedom (32). The data is relatively scattered; therefore, we choose a fit with a low number of parameters to be fitted. In fact, we choose a second-order fit (parabola shape, or in traffic engineering terms a Greenshields fundamental diagram), for which we fix the free-flow speed to the found value of 442 km/h. Moreover, in line with traffic engineering principles that no density yields no flow, we require the parabola to fit through (0,0). Now, two degrees of freedom have been set, which reduces the freedom in the fit to 1. The resulting parabola shape fit is shown in Figure 4 as well, and follows the point cloud nicely. The theoretical jam density found is $7.8E-4$ airplanes/ km^3 , and according to the model fit the highest flow would be found at $3.9E-4$ airplanes/ km^3 . That still is almost an order of magnitude below the maximum packing density of airplanes based on their minimum separation. Figure 6 shows the routes taken and shows that a large part of the space is unused. This is a 2D representation and indeed even in the used paths the full altitude range is not used either. This explains the lower density ranges.

In car traffic, the MFD was first hypothesized to strongly decrease for higher densities. Whereas that theoretically might indeed be the case, it turns out that for empirical MFDs, the congested branch is not complete and the production curve stops just beyond the critical density. This has been shown for most of the empirically found MFDs (15, 19). Also for air traffic, as expected, the MFD does not reach the top of the production, because air traffic is better planned and airplanes do not reduce their speed to standstill to queue. For some

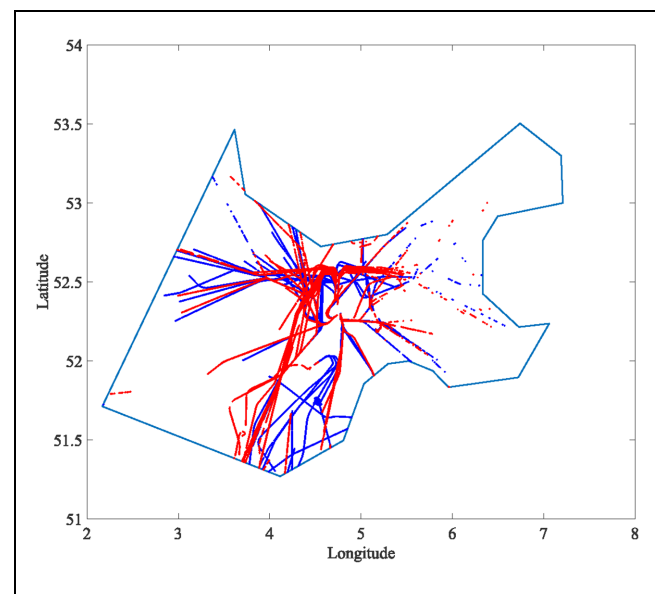


Figure 6. The routes of the airplane during one busy hour (two half hours are each shown in a different color).
Note: Color online only.

airports, such as London Heathrow, holding stacks are more common, and one might see a larger reduction in flow.

We consider efficiency with respect to the directness of the paths flown. Similar to the free-flow speed, we also define a free-flow efficiency, which shows the loss of efficiency also at low speeds. This is based on the ratio of the path lengths for the third to eighth percentile density range. This free-flow efficiency is slightly above 80%. Figure 7 shows the efficiency as function of the density. We also include a line that would have been the

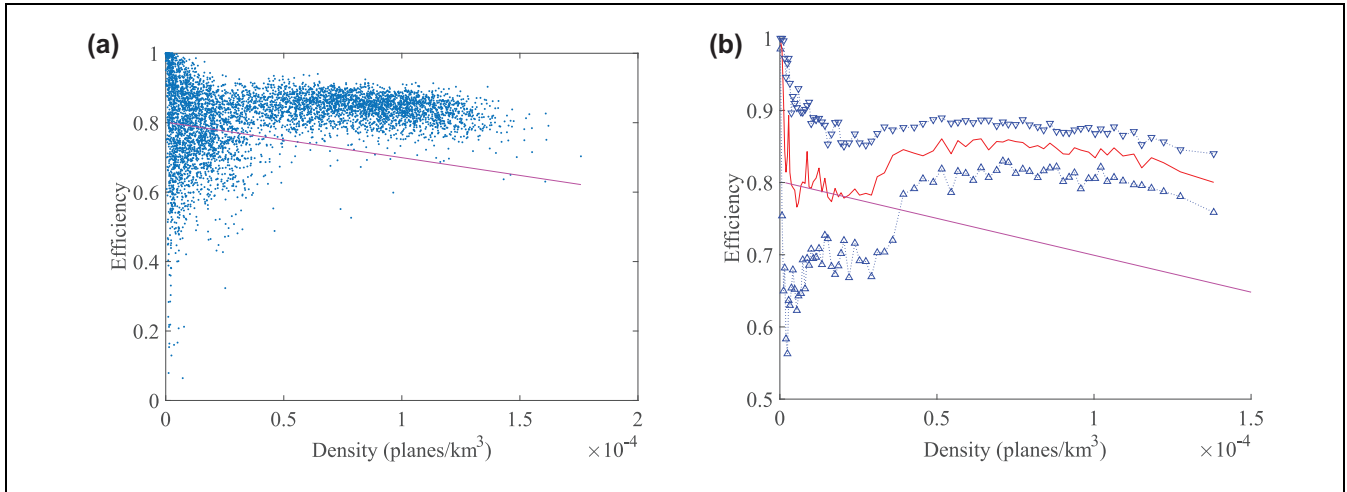


Figure 7. The efficiency of the airspace: (a) scatter and (b) line.

Note: Color online only.

efficiency if only speeds changed. This line is based on the Greenshields fundamental diagram, as fitted earlier in Figure 4. The figure shows that the flow reduction is much stronger than the reduction in efficiency, meaning that the reduction in production is largely caused by a reduction in speed. That is also visible by comparing Figure 7 with Figure 5a. The joint effect of reduction of speed and reduction of efficiency should cause the effect indicated by the magenta line. The reduction in free speed is much larger than the reduction of efficiency.

Figure 6 shows the routes airplanes take for a busy hour. It shows that the airplane trajectories spiral out, but as expected, mainly follow predefined paths instead of a uniform distribution over the available airspace. It is visible, for instance at the bottom, that some airplanes cross the CTA and are not departing or landing at Schiphol. This is shown in another way that airplanes are not too much in each other's paths, but they are mainly following the same streams.

Conclusions and Potential Applications

This research has presented a method to produce a meaningful MFD for air traffic. A crisp MFD occurs. We have seen that with higher densities of airplanes the effective speed reduces. Yet, the flow is still increasing and we do not reach (let alone exceed) densities for which maximum flow occurs, as observed in road traffic. The computed critical density for which that would happen, extrapolating a fitted Greenshields fundamental diagram, is two to three times the highest densities currently achieved.

These densities not being reached could be explained by various factors. Indeed, the area chosen is quite large compared to the area used for flying. A smaller area closer to the airport would possibly yield denser traffic,

but would also be even more structured and tightly controlled, as it would mainly involve airplanes in their final approach or initial departure to and from the runway. Also, high-density situations that would result in low speeds and potentially a decrease in flow are actively avoided by the air traffic controller. Two factors play a role here: airplanes cannot fly at very low speeds, and the comfort and efficiency of the airport. Through, for instance, ATFM regulations (resulting in ground holding), but also through holding stacks, a form of perimeter control is applied: air traffic control does not allow more airplanes into the controlled airspace than the airport and airspace can handle.

The MFD does show to which extent the speed reduces with higher loads. There can be various reasons for this speed reduction. It should not be used as way of comparatively assessing the airport or the air traffic control. Having said so, it would be interesting to see how they compare for various airports and find to which extent the shape (qualitatively and quantitatively) differs for different airports. Also, the underlying causes for these differences could help one to understand the effectiveness of airports, and potentially thereby improving their efficiency.

The current research has established a MFD based on empirical data from several months. It aggregated the data of all conditions. Indeed, several factors can influence this relationship, and given the empirical approach will have done so. Some factors to mention are as follows: severe weather limits the capacity of airports and runways, strong winds change ground speed as compared to air speed, and weather cells may cause the usable area of a sector to be reduced, or even cause flights to be rerouted to alternate airports. Also, in general, this study investigates CTA traffic in isolation,

even though in practice it has to be acknowledged that, for example, runways as limiting resources and spacing constraints that vary with aircraft performance (specified in wake turbulence categories) pose constraints on traffic flow in the terminal area, which in turn also affect traffic in the CTA. A follow-on study should further investigate the effect of these individual constraints, either data driven by separating the data in various classes or by simulation.

The MFD could potentially also be applied for determining the level of control for airspaces. We propose ideas here that are not reasonable to apply in current air transport, but might be—in future times—applicable for drone traffic. With many aircraft, decentralized control probably takes over individual conflict resolution. Air traffic control could be in the background up to the density that efficiency decreases with more than $X\%$; for higher densities, ATM would then start intervening. An option for this intervention could be a form of perimeter control where aircraft should stay out of a zone for as long as density is too high.

Author's Note

Minor textual changes were incorporated after a proofread by ChatGPT.

Author Contributions

The authors confirm contribution to the paper as follows: analyses and concepts – initiation: V. L. Knoop; analyses and concepts –performance: V. L. Knoop, M. ter Heide; contributions from the domain of airport and airplane operations: J. Ellerbroek; contributions from the overall field of transportation: S. Hoogendoorn; study conception and design: V. L. Knoop; data collection: V. L. Knoop; analysis and interpretation of results: V. L. Knoop, M. ter Heide, J. Ellerbroek S.P. Hoogendoorn ; draft manuscript preparation: V. L. Knoop. All authors reviewed the results and approved the final version of the manuscript.


Declaration of Conflicting Interests


The author(s) declared no potential conflicts of interest with respect to the research, authorship, and/or publication of this article.


Funding


The author(s) received no financial support for the research, authorship, and/or publication of this article.

ORCID iDs

Victor L. Knoop  <https://orcid.org/0000-0001-7423-3841>

Joost Ellerbroek  <https://orcid.org/0000-0002-2232-8299>

Mark ter Heide  <https://orcid.org/0000-0003-4351-9964>

Serge Hoogendoorn  <https://orcid.org/0000-0002-1579-1939>

References

1. Statistica, 2022. <https://www.statista.com/statistics/564717/airline-industry-passenger-traffic-globally/>.
2. Daganzo, C. Urban Gridlock: Macroscopic Modeling and Mitigation Approaches. *Transportation Research Part B: Methodological*, Vol. 41, No. 1, 2007, pp. 49–62.
3. Keyvan-Ekbatani, M., A. Kouvelas, I. Papamichail, and M. Papageorgiou. Exploiting the Fundamental Diagram of Urban Networks for Feedback-Based Gating. *Transportation Research Part B: Methodological*, Vol. 46, No. 10, 2012, pp. 1393–1403.
4. Doole, M., J. Ellerbroek, V. L. Knoop, and J. M. Hoekstra. Constrained Urban Airspace Design for Large-Scale Drone-Based Delivery Traffic. *Aerospace*, Vol. 8, No. 2, 2021, p. 38.
5. Cummings, C., and H. S. Mahmassani. Measuring the Impact of Airspace Restrictions on Air Traffic Flow Using Four-Dimensional System Fundamental Diagrams for Urban Air Mobility. *Transportation Research Record: Journal of the Transportation Research Board*, 2023. 2677: 1012–1026.
6. Aarts, M. J., J. Ellerbroek, and V. L. Knoop. Capacity of a Constrained Urban Airspace: Influencing Factors, Analytical Modelling and Simulations. *Transportation Research Part C: Emerging Technologies*, Vol. 152, 2023, p. 104173.
7. Cummings, C., and H. Mahmassani. Emergence of 4D System Fundamental Diagram in Urban Air Mobility Traffic Flow. *Transportation Research Record: Journal of the Transportation Research Board*, 2021. 2675: 841–850.
8. Tereshchenko, I., M. Hanson, and B. Zou. Macroscopic Fundamental Diagram for Air Traffic: Preliminary Theoretic Results and Simulation Findings. *Proc., International Conference for Research in Air Transportation, (virtual)*, Tampa, FL, 2020.
9. Haddad, J., B. Mirkin, and K. Assor. Traffic Flow Modeling and Feedback Control for Future Low-Altitude Air City Transport: An MFD-Based Approach. *Transportation Research Part C: Emerging Technologies*, Vol. 133, 2021, p. 103380.
10. Geroliminis, N., and C. F. Daganzo. Existence of Urban-Scale Macroscopic Fundamental Diagrams: Some Experimental Findings. *Transportation Research Part B: Methodological*, Vol. 42, No. 9, 2008, pp. 759–770.
11. Edie, L. Discussion of Traffic Stream Measurements and Definitions. *Proc., Second International Symposium on the Theory of Traffic Flow*, OECD, Paris, France, 1965.
12. Administration, F. A. *JO 7210.3DD -Facility Operation and Administration – Traffic Management – National, Center, and Terminal Ground Delay Programs*, 2023.
13. Godfrey, J. The Mechanism of a Road Network. *Traffic Engineering and Control*, Vol. 11, No. 7, 1969, pp. 323–327.
14. Mahmassani, H., J. C. Williams, and R. Herman. Investigation of Network-Level Traffic Flow Relationships: Some Simulation Results. *Transportation Research Record: Journal of the Transportation Research Board*, 1984. 971: 121–130.
15. Knoop, V. L., and S. P. Hoogendoorn. Empirics of a Generalized Macroscopic Fundamental Diagram for Urban Freeways. *Transportation Research Record: Journal of the Transportation Research Board*, 2013. 2391: 133–141.

16. Knoop, V. L., P. B. van Erp, L. Leclercq, and S. P. Hoogendoorn. Empirical MFDs Using Google Traffic Data. *Proc., 21st International Conference on Intelligent Transportation Systems (ITSC)*, Maui, HI, IEEE, New York, 2018, pp. 3832–3839.
17. Du, J., H. Rakha, and V. V. Gayah. Deriving Macroscopic Fundamental Diagrams from Probe Data: Issues and Proposed Solutions. *Transportation Research Part C: Emerging Technologies*, Vol. 66, 2016, pp. 136–149.
18. Ambühl, L., and M. Menendez. Data Fusion Algorithm for Macroscopic Fundamental Diagram Estimation. *Transportation Research Part C: Emerging Technologies*, Vol. 71, 2016, pp. 184–197.
19. Loder, A., L. Ambühl, M. Menendez, and K. W. Axhausen. Understanding Traffic Capacity of Urban Networks. *Scientific Reports*, Vol. 9, No. 1, 2019, pp. 1–10.
20. Gayah, V. V., and C. F. Daganzo. Clockwise Hysteresis Loops in the Macroscopic Fundamental Diagram: An Effect of Network Instability. *Transportation Research Part B: Methodological*, Vol. 45, No. 4, 2011, pp. 643–655.
21. Hani Mahmassani, M. S., and A. Zockaie. Urban Network Gridlock: Characteristics, Dynamics and Control. *Proc., 20th International Symposium of Transportation and Traffic Theory*, Noordwijk, The Netherlands, 2013.
22. Cuniasse, P.-A., C. Buisson, J. Rodriguez, E. Teboul, and D. De Almeida. Analyzing Railroad Congestion in a Dense Urban Network Through the Use of a Road Traffic Network Fundamental Diagram Concept. *Public Transport*, Vol. 7, No. 3, 2015, pp. 355–367.
23. Hoogendoorn, S. P., W. Daamen, V. L. Knoop, J. Steenbakkens, and M. Sarvi. Macroscopic Fundamental Diagram for Pedestrian Networks: Theory and Applications. *Transportation Research Procedia*, Vol. 23, 2017, pp. 480–496.
24. Johari, M., M. Keyvan-Ekbatani, L. Leclercq, D. Ngoduy, and H. S. Mahmassani. Macroscopic Network-Level Traffic Models: Bridging Fifty Years of Development Toward the Next Era. *Transportation Research Part C: Emerging Technologies*, Vol. 131, 2021, p. 103334.
25. Knoop, V. L., S. P. Hoogendoorn, and J. W. C. Van Lint. Routing Strategies Based on Macroscopic Fundamental Diagram. *Transportation Research Record: Journal of the Transportation Research Board*, 2012. 2315: 1–10.
26. Hajiahmadi, M., V. L. Knoop, B. De Schutter, and H. Hellendoorn. Optimal Dynamic Route Guidance: A Model Predictive Approach Using the Macroscopic Fundamental Diagram. *Proc., 16th International IEEE Conference on Intelligent Transportation Systems (ITSC 2013)*, The Hague, Netherlands, IEEE, New York, 2013, pp. 1022–1028.
27. Geroliminis, N., J. Haddad, and M. Ramezani. Optimal Perimeter Control for Two Urban Regions with Macroscopic Fundamental Diagrams: A Model Predictive Approach. *IEEE Transactions on Intelligent Transportation Systems*, Vol. 14, No. 1, 2013, pp. 348–359.
28. Yuan, J., C. Wu, K. L. Teo, S. Zhao, and L. Meng. Perimeter Control with State-Dependent Delays: Optimal Control Model and Computational Method. *IEEE Transactions on Intelligent Transportation Systems*, Vol. 23, No. 11, 2022, pp. 20614–20627.
29. Daganzo, C., V. Gayah, and E. Gonzales. Macroscopic Relations of Urban Traffic Variables: Bifurcations, Multivaluedness and Instability. *Transportation Research Part B: Methodological*, Vol. 45, No. 1, 2011, pp. 278–288.
30. Schiphol Amsterdam Airport, 2022. <https://www.schiphol.nl/en/schiphol-group/page/transport-and-traffic-statistics/>.
31. Ministerie van Infrastructuur en Milieu; Dutch Ministry of Infrastructure and Environment. *Luchtruimvisie (vision on the airspace, in Dutch)*. The Hague, 2012.
32. Knoop, V. L., and W. Daamen. Automatic Fitting Procedure for the Fundamental Diagram. *Transportmetrica B: Transport Dynamics*, Vol. 5, No. 2, 2017, pp. 129–144.